Synthesis and characterization of $(Ba,Ca)TiO_3$ - $(Ni,Co,Zn)Fe_2O_4$ multiferroic particulate composite

Richa Sharma[1], N. C. Mehra[2], R. P. Tandon[1,*]

[1]*Department of Physics and Astrophysics, University of Delhi, Delhi 110007, India*
[2]*Department of Geology, University of Delhi, Delhi 110007, India*

[*]Corresponding author, Tel: (+91) 9818229608; E-mail: ram_tandon@hotmail.com

Received: 31 March 2016, Revised: 08 August 2016 and Accepted: 29 December 2016

DOI: 10.5185/amp.2017/408
www.vbripress.com/amp

Abstract

In the present work, the composite series (1-x) $Ba_{0.94}Ca_{0.06}TiO_3$ - (x) $Ni_{0.7}Co_{0.1}Zn_{0.2}Fe_2O_4$ (where x = 0.1, 0.2, 0.3 and 0.4 wt. fraction) was synthesized by solid state reaction method followed by conventional sintering. The structure and morphology of prepared samples were examined using X-ray diffractometer (XRD) and scanning electron microscopy (SEM), respectively. In addition, dielectric constant (ε') and loss tangent (tan δ) of prepared samples were measured as a function of frequency and temperature. The room temperature values of dielectric constant (ε') of composite samples are found to decrease from 529.29 to 159.52 as ferrite content increased from x = 0.1 to x = 0.4 at 1 kHz frequency. Moreover, in the dielectric constant vs. temperature plots of the composite samples, ferroelectric to paraelectric phase transition of pure $Ba_{0.94}Ca_{0.06}TiO_3$ is observed. Furthermore, ferroelectric and magnetic properties of the composite samples were studied at room temperature. With increasing addition of the ferrite content in the composites, the ferroelectric properties get weakened and the magnetic behavior of the composite samples improved. The maximum values of saturation magnetization (M_s) and remanant magnetization (M_r) are 22.52 emu/gm and 3.39 emu/gm, respectively, for composite sample containing 0.4 wt. fraction $Ni_{0.7}Co_{0.1}Zn_{0.2}Fe_2O_4$.

Keywords: Composite materials, ferroelectric, dielectric properties, magnetic properties, ferrite.

Introduction

Multiferroic composites consisting of ferroelectric and magnetic materials, is a novel class of multifunctional materials which have attracted a great deal of attention worldwide in the past few years from academics as well as from technology perspective due to increasing demand of electronic device miniaturization and multi-functionality **[1-3]**. These composites exhibit magnetoelectric (ME) effect in which magnetization can be induced by the application of electric field and electric polarization can be induced by the application of magnetic field and find potential applications as phase shifters, memory devices, spintronic devices, current sensors, etc **[1, 4]**. So far most of the multiferroic composite systems that have shown high ME performance used lead based ferroelectric materials **[5, 6]**. But, due to concerns regarding pollution of environment and its toxicity to human beings, lead free materials are preferred. Thus, intensive research has been undertaken worldwide to develop high ME response lead-free multiferroic composites.

Lead free barium titanate ($BaTiO_3$) is a well-known perovskite ferroelectric material that has been selected as the ferroelectric phase in numerous multiferroic particulate composites **[7, 8]**. Further, strategic substitution at Ba and/or Ti sites in $BaTiO_3$ (BT) has also been performed to effectively control its ferroelectric and dielectric properties. It is reported in the literature that calcium (Ca) substituted at Ba site not only improves the temperature stability of the piezoelectric and dielectric properties of BT, but also reduces the chance of formation of hexagonal phase that is not ferroelectric **[9, 10]**. However, in the literature there are very few reports on the multiferroic composite system employing Ca substituted $BaTiO_3$ as the ferroelectric phase. Sadhana et al. **[11]** examined the magnetic field induced polarization and ME effect in $Ba_{0.94}Ca_{0.06}TiO_3$ - $Ni_{0.7}Co_{0.1}Zn_{0.2}Fe_2O_4$ ferrite nanocomposites synthesized by using sol-gel method with maximum value of ME coefficient achieved is 280 mV/cm Oe. Puli et al. **[12]** studied the structural, morphological, ferroelectric and ferromagnetic properties of the $Ba_{0.7}Ca_{0.3}TiO_3$ - $BaFe_{0.2}Ti_{0.8}O_3$ multiferroic composites and reported the enhanced ferroelectric properties while maintaining the ferromagnetic properties. For the magnetic phase of the multiferroic composites, $Ni_{0.7}Co_{0.1}Zn_{0.2}Fe_2O_4$ (NCZF) has been selected. It is reported in the literature that Zn substituted $NiFe_2O_4$ exhibits high saturation magnetization and resistivity **[13-15]**. Also, $NiFe_2O_4$ substituted with Co possesses large magnetostriction coefficient and resistivity **[16, 17]**.

Keeping the above facts in mind, in the present investigation, multiferroic particulate composite system $Ba_{0.94}Ca_{0.06}TiO_3$ - $Ni_{0.7}Co_{0.1}Zn_{0.2}Fe_2O_4$ has been synthesized by solid state reaction method. The phase formation and morphology of the samples have been examined. In addition, the dielectric, ferroelectric and magnetic properties of the composites have been investigated.

Experimental

Materials/ chemical details

To fabricate multiferroic composite series (1-x) $Ba_{0.94}Ca_{0.06}TiO_3$ - (x) $Ni_{0.7}Co_{0.1}Zn_{0.2}Fe_2O_4$ (where x = 0.1, 0.2, 0.3 and 0.4 wt. fraction), pure ferroelectric phase $Ba_{0.94}Ca_{0.06}TiO_3$ (BCT) and magnetic phase $Ni_{0.7}Co_{0.1}Zn_{0.2}Fe_2O_4$ (NCZF) were first synthesized by conventional solid state reaction method. To prepare BCT, $BaCO_3$, $CaCO_3$ and TiO_2 with purity > 99% procured from Sigma Aldrich, USA were mixed in stoichiometric ratio using ball milling in distilled water with zirconia media. For the preparation of NCZF, analytical grade Fe_2O_3, CoO, ZnO and NiO with purity > 99% procured from Sigma Aldrich, USA were also mixed in stoichiometric ratio using ball milling in isopropyl alcohol (IPA) with zirconia media.

Characterizations

The thoroughly mixed raw materials of the BCT and NCZF phases were dried in oven followed by calcination at 1100 ^oC and 1150 ^oC, respectively for 6 hrs. Further, the calcined powders of the ferroelectric and ferrite phases were mixed together in different weight ratios and then compacted into circular pellets using hydraulic press. The green pellets of the composite samples were sintered in air at 1200 ^oC for 6 hrs. Hereafter, composites are abbreviated as S1, S2, S3 and S4 corresponding to x = 0.1, 0.2, 0.3 and 0.4 wt. fraction, respectively of the magnetic phase content.

The prepared samples were lapped to a thickness of ~1 mm using silicon carbide abrasive powder followed by cleaning using an ultrasonicator. The phase formation of the composite samples was analyzed by X-ray diffractometer (XRD, Rigaku Miniflex II) equipped with Cu Kα radiation (λ = 1.5406 Å). The fractured surface of the sintered samples was examined by scanning electron microscope (SEM; Jeol JSM 6610LV). The density of the samples was determined by Archimedes principle. The dielectric behavior of the composite samples was also studied as a function of frequency and temperature using an impedance analyzer (Wayne kerr 6500B). Furthermore, the ferroelectric and magnetic properties of the composites samples were recorded at room temperature using automatic *P* - *E* loop tracer based on Sawyer-Tower circuit and Vibrating Sample Magnetometer, respectively.

Results and discussion

Phase and microstructural analysis

X-ray diffraction (XRD) analysis of the composite samples is done and corresponding plot is shown in **Fig. 1**.

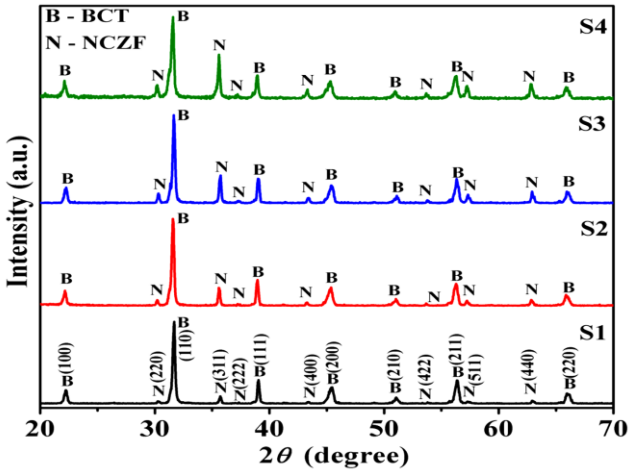

Fig. 1. X-ray diffraction (XRD) patterns of the composite samples.

All the diffraction peaks observed in the XRD patterns of the composite samples presented in **Fig. 1** either belongs to the BCT phase or to the NCZF phase, indicating that both the constituent phases coexist in composite and no impurity peak was detected within the detection limit of the XRD. The diffraction peaks are indexed using the standard powder diffraction data for NCZF (JCPDS file no. 74-2081) and BCT (JCPDS file no. 05-0626). The intensity of the peak corresponding to the NCZF phase increases with its increasing content in the composites.

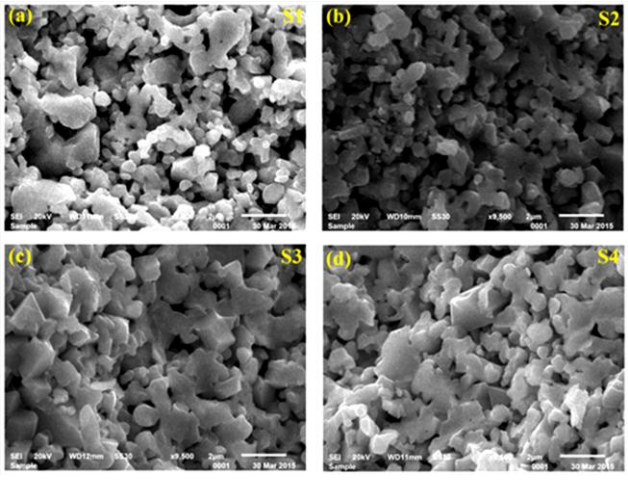

Fig. 2. SEM of the fractured surface of the composite samples (a) S1, (b) S2, (c) S3 and (d) S4.

Fig. 2 shows the SEM images of the fractured surface of the composite samples. The grains of the NCZF phase are homogeneously distributed among the BCT phase. Besides, the presence of slight porosity in the composite

samples is evident from the micrographs. The values of average grain size for the samples S1, S2, S3 and S4 are 0.90, 0.93, 1.38 and 1.48 μm, respectively. The values of density of the composite samples S1, S2, S3 and S4 are 4.78, 4.96, 4.61 and 4.68 g/cm^3, respectively.

Dielectric properties

Frequency dependence of dielectric properties

The dielectric properties of the prepared composite samples have been measured as a function of frequency at room temperature and corresponding plots are presented in **Fig. 3**. From the plot shown in **Fig. 3(a)**, it can be noted that for all composite samples dielectric constant (ε') decreases with increase in frequency and then attains almost constant values at higher frequencies, indicating usual dielectric dispersion which can be explained on the basis of Maxwell-Wagner interfacial polarization and Koops theory **[18]**.

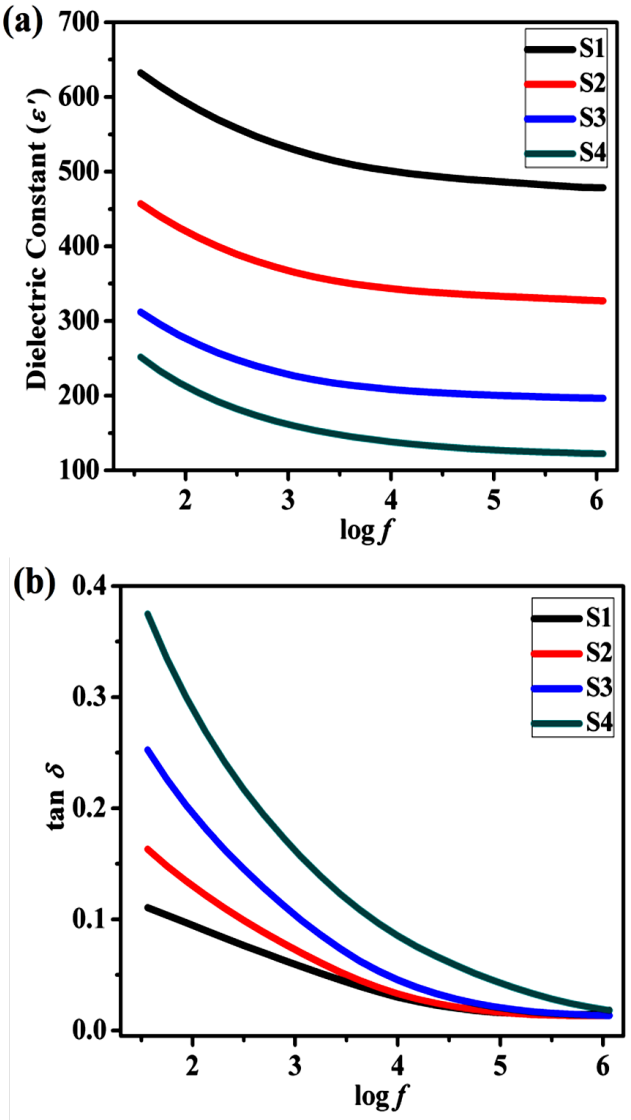

Fig. 3. Variation of (a) dielectric constant (ε') and (b) loss tangent (tan δ) of composite samples as a function of frequency at room temperature.

Different types of polarizations contribute to dielectric constant values at low frequencies. But, in the high frequency side, some of these polarizations are not able to follow the variation of the applied electric field and hence, contribute less to dielectric constant. Furthermore, with increase in NCZF content in the composite samples, dielectric constant is found to decrease. Composite sample S1 exhibits the maximum dielectric constant, while, sample S4 possesses the minimum dielectric constant in the entire measured frequency range. The observed decrease in the dielectric constant values with NCZF content can be attributed to the lower dielectric constant of the NCZF phase in comparison to the BCT phase **[19]**. **Fig. 3(b)** shows the variation of loss tangent (tan δ) as a function of frequency of the composite samples. An increase in the tan δ with increase in the ferrite content from 10 wt% to 40 wt% in the composites is clearly evident from the plot. This might be due to the lower resistivity of the NCZF phase in comparison to the BCT phase which offers leakage path to the stored charge.

Temperature dependence of dielectric properties

Fig. 4 shows the variation of the dielectric constant (ε') and loss tangent (tan δ) of composite samples as function of temperature at two extreme frequencies i.e. 1 KHz and 1 MHz. For all the composite samples, the ferroelectric to paraelectric phase transition is observed in the temperature range 144 to 150 ^{o}C, which is higher than the value reported for the pure BCT phase **[20]**. Similar results have been reported in the literature by other researchers **[21]**. The observed changes in the transition temperature might be related to the diffusion of ions between the constituent phases *i.e.* BCT and NCZF during the sintering process **[22]**. Furthermore, for samples S1 and S2, the transition peak is clearly visible at both the extreme frequencies, indicating that for low ferrite content ($x \leq 0.2$) dielectric behavior is governed by the BCT phase, while, the effect of NCZF can be noted at high temperature in ε' and tan δ. For the sample S3 and S4 the transition peak seems to be suppressed at low frequency 1 KHz. For samples containing NCZF content higher than 20 wt%, the influence of ferrite phase is considerable on the dielectric properties and a continuous increase in the dielectric constant values for the sample S3 and S4 can be noticed at low frequency 1 kHz from the plot (**Fig. 4(a)**). At frequency 1 kHz, for the samples S3 and S4, the transition peak is covered by the conduction contribution from the NCZF phase and only a weak peak can be observed at high frequency 1MHz (**Fig. 4(b)**) **[23]**. The variation of tan δ of the composite samples is shown in **Fig. 4(c)** and **Fig. 4(d)**. An increase in tan δ with increase in temperature is observed for all the prepared composite samples due to the decreasing resistivity of the composite samples with rise in temperature **[24]**.

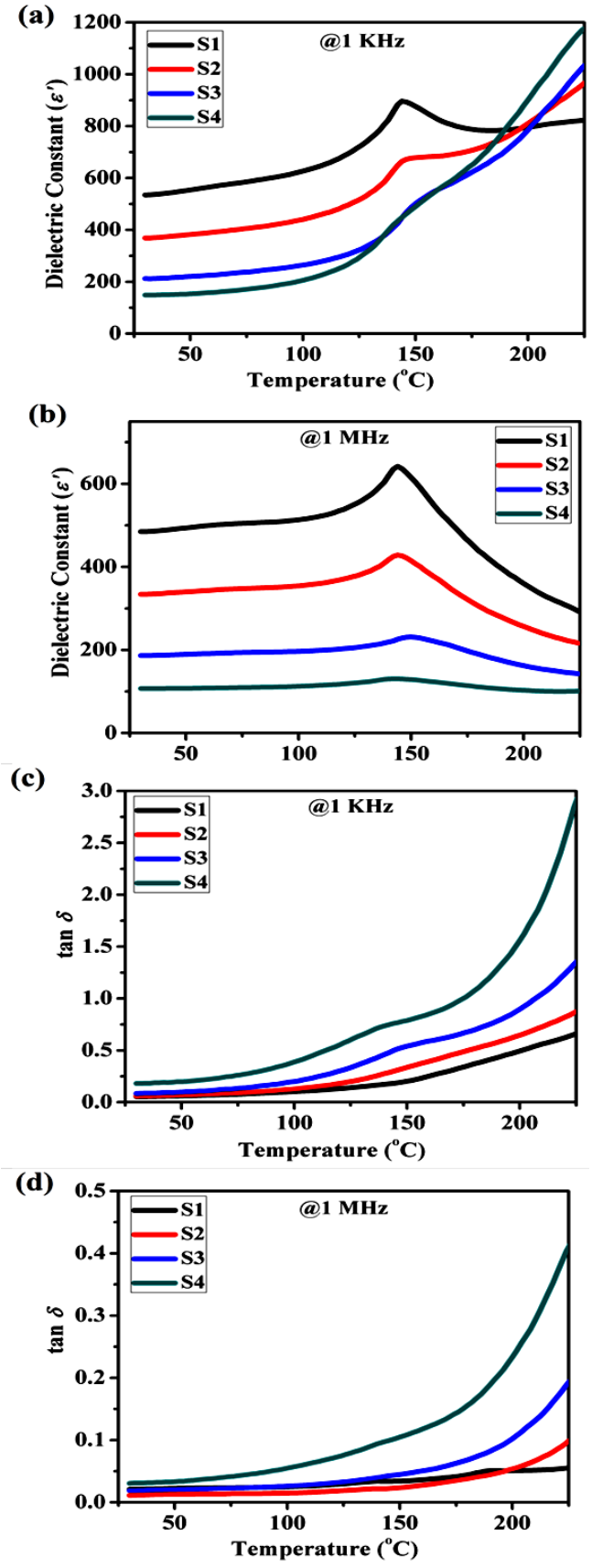

Fig. 4. Variation of dielectric constant (ε') of composite samples at selected frequencies (a) 1 KHz and (b) 1 MHz. Variation of loss tangent (tan δ) of composite samples at selected frequencies (c) 1 KHz and (d) 1 MHz.

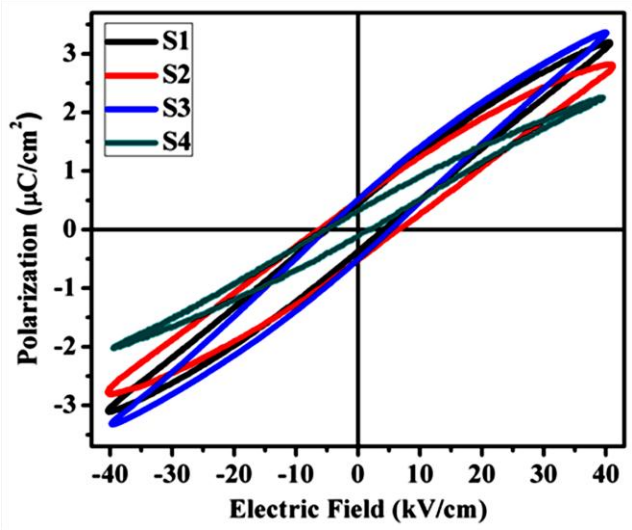

Fig. 5. Polarization (P) vs. electric field (E) loops of the composite samples at room temperature.

Ferroelectric properties

The ferroelectric properties of the composite samples have been studied by recording the polarization (P) *vs.* electric field (E) loops at room temperature. **Fig. 5** represents the P - E loops of the composite samples. It can be noticed from the plot that obtained loops are not saturated. A significant effect of content of the individual phases has been noticed on the maximum polarization (P_{max}), remanant polarization (P_r) and coercive field (E_c) values of the composite samples.

The value of maximum polarization (P_{max}) is found to decrease with increasing ferrite content from 3.19 μC/cm^2 for sample S1 to 2.23 μC/cm^2 for the sample S4, except for the sample S3 for which P_{max} is 3.36 μC/cm^2. The observed high value of P_{max} for the sample S3 may be attributed to the space charge effect in the composite **[25]**. Furthermore, the decrease in P_{max} values of the samples may be due to the presence of ferrite phase that results in the dilution of the ferroelectric properties. The value of coercive field for the composite samples S1, S2, S3 and S4 are 4.51, 6.27, 5.22 and 3.35 kV/cm, respectively. The decrease in E_c values from the sample S2 to S4 indicates that the composite samples are becoming more easily polarized by the application of electric field **[26]**. Similar behavior has been reported in the literature for other composite systems **[27]**. In addition, the P - E loops of the composite samples are found to be unsymmetrical about the origin which may be ascribed to the internal electric field originating from the short distance, off-center and inherent movement of bound electrons **[28]**.

Magnetic properties

The magnetic properties of the composite samples have been investigated by recording the magnetization (M) vs. magnetic field (H) loops at room temperature. The M - H plots obtained for the composite samples are shown in **Fig. 6**, demonstrating the presence of an ordered magnetic structure.

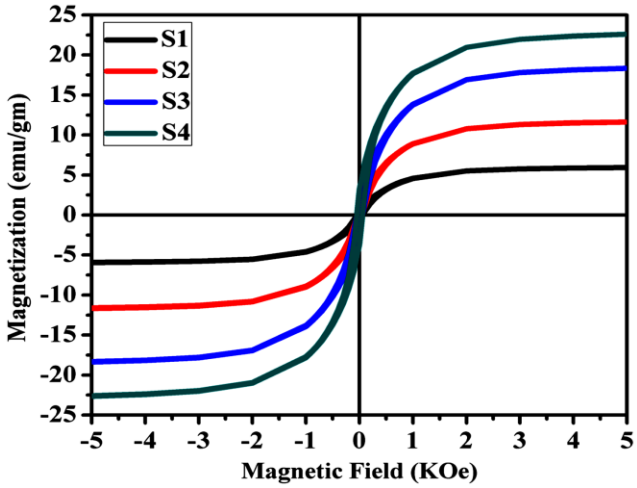

Fig. 6. Magnetization (*M*) vs. Magnetic field (*H*) loops of the composite samples at room temperature.

Clearly, all samples show the saturated magnetic hysteresis loops. The saturation magnetization (M_s) and remanant magnetization (M_r) is found to increase with increase in the NCZF content in the composites. This behavior can be explained by the fact that individual ferrite particles contribute to the magnetization and M_s is given by vector sum of all these individual contributions **[29]**. With increasing NCZF content in the composites, the magnetic contacts increase that result in net increase in the magnetization. The presence of nonmagnetic BCT phase in the composite behave as pores in the presence of magnetic field and break the magnetic circuit, which result in the degradation of the magnetic properties **[30]**. The values of M_s, M_r and H_c varies from 5.92 emu/gm, 0.51 emu/gm and 49.37 Oe, respectively for the sample S1 to 22.52 emu/gm, 3.39 emu/gm and 52.70 Oe, respectively for the sample S4. The coercive field (H_c) of the composite samples first increases as ferrite content increase up to 30 wt% and then decreases slightly for composite sample containing ferrite content higher than 30 wt%.

Conclusion

In summary, the multiferroic composite series (1-x) $Ba_{0.94}Ca_{0.06}TiO_3$ - (x) $Ni_{0.7}Co_{0.1}Zn_{0.2}Fe_2O_4$ (where x = 0.1, 0.2, 0.3 and 0.4 wt. fraction) is successfully prepared by solid state reaction method followed by conventional sintering. XRD analysis confirmed the formation of cubic spinel structure for the NCZF and tetragonal structure for the BCT. A considerable effect of ferrite content on the dielectric properties of the prepared samples is observed. In addition, all samples at room temperature exhibit *M* - *H* and *P* - *E* loops, showing simultaneously, ferroelectric and magnetic properties.

Acknowledgements

One of the authors (Richa Sharma) is thankful to the University Grants Commission (UGC), New Delhi, India for providing the research fellowship.

References

1. Nan, C.-W.; Bichurin, M. I.; Dong, S.; Viehland, D.; Srinivasan, G.; *J. Appl. Phys.*, **2008**, *103*, 031101.
2. Wang, Y.; Hu, J.; Lin, Y.; Nan, C.-W.; *NPG Asia Mater.*, **2010,** *2*, 61.
3. Vaz, C. A. F.; Hoffman, J.; Ahn, C. H.; Ramesh, R.; *Adv. Mater.*, **2010**, *22*, 2900.
4. Vopson, M. M.; *Crit. Rev. Solid State Mater. Sci.*, **2014,** *0*, 1.
5. Ryu, J.; Priya, S.; Carazo, A. V.; Uchino, K.; Kim, H.-E.; *J. Am. Ceram. Soc.*, **2001,** *84*, 2905.
6. Zeng, M.; Wan, J. G.; Wang, Y.; Yu, H.; Liu, J.-M.; Jiang, X. P.; Nan, C. W.; *J. Appl. Phys.*, **2004**, *95*, 8069.
7. Ren, S. Q.; Weng, L. Q.; Song, S.-H.; Li, F.; Wan, J. G.; Zeng, M.; *J. Mater. Sci.*, **2005**, *40*, 4375.
8. Sreenivasulu, G.; Babu, V. H.; Markandeyulu, G.; Murty, B. S.; *Appl. Phys. Lett.*, **2009**, *94*, 112902.
9. Victor, P.; Ranjith, R.; Krupanidhi, S. B.; *J. Appl. Phys.*, **2003,** *94*, 7702.
10. Jaffe, B.; Cook Jr., W. R.; Jaffe, H.; Piezoelectric Ceramics; Academic Press, **1971**.
11. Sadhana, K.; Murthy, S. R.; Jie, S.; Xie, Y.; Liu, Y.; Zhan, Q.; Li, R.-W.; *J. Appl. Phys.*, **2013**, *113*, 17C731.
12. Puli, V. S.; Coondoo, I.; Panwar, N.; Srinivas, A.; Katiyar, R. S.; *J. Appl. Phys.*, **2012**, *111*, 102802.
13. Uskokovi, V.; Drofenik, M.; Ban, I.; *J. Magn. Magn. Mater.*, **2004**, 284, 294.
14. Rahimi, M.; Kameli, P.; Ranjbar, M.; Hajihashemi, H.; Salamati, H.; *J. Mater. Sci.*, **2013**, *48*, 2969.
15. Atif, M.; Nadeem, M.; Grossinger, R.; Turtelli, R. S.; *J. Alloy. Compd.*, **2011**, *509*, 5720.
16. Devan, R. S.; Ma, Y.-R.; Chougule, B. K.; *Mater. Chem. Phys.*, **2009**, *115*, 263.
17. Devan, R. S.; Kolekar, Y. D.; Chougule, B. K.; *J. Phys.: Condens. Matter.*, **2006**, *18*, 9809.
18. Koops, C. G.; *Phys. Rev.*, 1951, *83*, 121.
19. Ramanaa, M. V.; Reddy, N. R.; Sreenivasulu, G.; Kumar, K. V. S.; Murty, B. S.; Murthy, V. R. K.; *Curr. Appl. Phys.*, **2009**, *9*, 1134.
20. Sonia, Patel, R. K.; Prakash, C.; Kumar, P.; *J. Ceram. Process. Res.*, **2011**, *12*, 634.
21. Gupta, A.; Chatterjee, R.; *J. Eur. Ceram. Soc.*, **2013,** *33*, 1017.
22. Maier, R.; Cohn, J. L.; Neumeier, J. J.; Bendersky, L. A.; *Appl. Phys. Lett.*, **2001**, *78*, 2536.
23. Yu, Z.; Ang, C.; *J. Appl. Phys.*, **2002**, *91*, 794.
24. Fawzi, A. S.; Sheikh, A. D.; Mathe, V. L.; *J. Alloy. Compd.*, **2010**, *493*, 601.
25. Zheng, R. Y.; Wang, J.; Ramakrishna, S.; *J. Appl. Phys.*, **2008,** *104*, 034106.
26. Sheikh, D.; Mathe, V. L.; *Smart Mater. Struct.*, **2009**, *18*, 065014.
27. Pradhan, D. K.; Chowdhury, R. N. P.; Nath, T. K.; *Appl. Nanosci.*, **2012,** *2*, 261.
28. Ciomaga, C. E.; Neagu, A. M.; Pop, M. V.; Airimioaei, M.; Tascu, S.; Schileo, G.; Galassi, C.; Mitoseriu, L.; *J. Appl. Phys.*, **2013**, *113*, 074103.
29. Mudinepalli, V. R.; Song, S. H.; Murty, B. S.; *Scripta Mater.*, **2014**, *82*, 9.
30. Babu, S. N.; Min, S. G.; Malkinski, L.; *J. Appl. Phys.*, **2011,** *109*, 07D911.

